

## Weak Interactions Dominating the Supramolecular Self-Assembly in a Salt: A Designed Single-Crystal-to-Single-Crystal Topochemical Polymerization of a Terminal Aryldiacetylene

Zhong Li, Frank W. Fowler, and Joseph W. Lauher\*

*Department of Chemistry, State University of New York, Stony Brook, New York, 11794-3400*

Received August 25, 2008; E-mail: jlauher@notes.cc.sunysb.edu

**Abstract:** Single-crystal-to-single-crystal (SCSC) topochemical polymerizations of diacetylenes can yield nearly defect-free conjugated polymer crystals unattainable by other methods. Aryl-substituted diacetylenes with their potentially greater conjugation have been targeted for years, but until now no one has reported a SCSC polymerization of any aryl-substituted diacetylene. This is presumably due to the rigidity of such diaryl-substituted monomers as well as the lack of control over the supramolecular structure. To address this problem, the polymerization of a terminal phenyldiacetylene was targeted. It was assumed that a terminal diacetylene should demonstrate greater flexibility in the solid state. To establish the necessary (~4.9 Å) repeat distance, commensurate with the repeat distance in the polymer, a host–guest system was designed. The chosen diacetylene guest, the amine **DABzNH<sub>2</sub>**, was to be crystallized with the oxalamide dicarboxylic acid host, **H<sub>2</sub>og**. The plan required a segregation of the hydrogen bonds, amide–amide hydrogen bonds to establish the 4.9 Å spacing, and the carboxylate to ammonium ion hydrogen bonds to organize the guest. Prior to carrying out the diacetylene synthesis a series of model salts were studied. Consistent with the hydrophobic effect it was found that amines with large “greasy” substituents assembled according to the design. Once the model studies established that weak interactions could dominate the supramolecular structure of a salt, the actual design was put to the test. The targeted guest, **DABzNH<sub>2</sub>**, was synthesized and crystals of the host–guest salt (**DABzNH<sub>3</sub>)<sub>2</sub>og** were prepared. The resulting crystal structure was in complete accordance with the design. A SCSC polymerization was achieved by a slow annealing treatment lasting about three months. The crystal structure of the resulting polymer not only confirmed the first example of a poly(aryldiacetylene) single crystal, it also revealed an unexpected reaction pathway that shows a major movement involving the rigid aromatic substituent.

### Introduction

Topochemical polymerizations are reactions that take place in a condensed phase with the structure of the product determined by the prearrangement of the reactant monomers in space.<sup>1,2</sup> This nonclassical polymerization method can lead to products otherwise unobtainable and also to a more insightful understanding of reaction pathways. More importantly, when such reactions proceed within a single-crystal-to-single-crystal (SCSC) environment, control of the stereo and regiochemistry in the corresponding polymer should be absolute. Therefore, one has a unique opportunity to map out exact reaction trajectories<sup>3</sup> and obtain outstanding functional materials with highly ordered polymer structures.<sup>4</sup> In particular, topochemical polymerizations have been shown to be the only efficient way

of preparing polydiacetylenes (PDAs), as was pioneered by Wegner in 1969.<sup>2</sup> The X-ray diffraction data from the PDA single crystals also helped to confirm the controversial ene-yne type backbone structure in the early days of the field.<sup>5</sup>

The typical topochemical requirements for diacetylene polymerization in crystalline state are known to be as follows:<sup>6</sup> The monomers need to be spaced ~4.9 Å apart, a separation equal to the repeat distance in the corresponding polymer. An angle between the axis of the array and the diacetylene rod of 45° will bring the C1 and C4 reactive centers of neighboring diacetylenes into a van der Waals contact of 3.5 Å (Figure 1). The fulfillment of these structural parameters increases the likelihood of maintaining the crystalline lattice during the entire transformation by minimizing the structural changes associated with polymerization. The difficulty is the fact that most diacetylenes do not crystallize in accordance with these structural parameters. If a given compound does not crystallize properly, there is little one can do to change the crystal structure of a

- (1) (a) Hasegawa, M. *Chem. Rev.* **1983**, *83*, 507–518. (b) Ogawa, T. *Prog. Polym. Sci.* **1995**, *20*, 943–985. (c) Matsumoto, A.; Odani, T. *Macromol. Rapid Commun.* **2001**, *22*, 1195–1215. (d) Matsumoto, A. *Top. Curr. Chem.* **2005**, *254*, 263–305. (e) Itoh, T. *Polymer* **2005**, *46*, 6998–7017.
- (2) Wegner, G. *Z. Naturforsch., B* **1969**, *24*, 824–832.
- (3) (a) Furukawa, D.; Matsumoto, A. *Macromolecules* **2007**, *40*, 6048–6056. (b) Matsumoto, A.; Furukawa, D.; Mori, Y.; Tanaka, T.; Oka, K. *Cryst. Growth Des.* **2007**, *7*, 1078–1085. (c) Furukawa, D.; Kobatake, S.; Matsumoto, A. *Chem. Commun.* **2008**, 55–57.

- (4) Ed.: Skotheim, T. A.; Elsenbaumer, R. L.; Reynolds, J. R. *Handbook of Conducting Polymers*, 2nd edition; Marcel Dekker: New York, 1998.
- (5) Apgar, P. A.; Yee, K. C. *Acta Crystallogr., Sect. B* **1978**, *34*, 957–959.
- (6) Baughman, R. H. *J. Polym. Sci., Polym. Phys. Ed.* **1974**, *12*, 1511–1535.

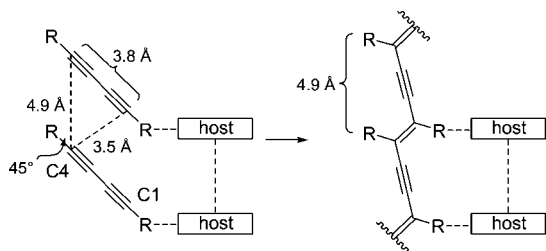


**Figure 1.** Topochemical requirements for diacetylene polymerization and the host-guest strategy of aligning diacetylenes for such requirements.

pure substance. Thus, SCSC diacetylene polymerizations are somewhat a matter of chance and far from common place.

In previous work, we have used a host-guest cocrystal approach to establish these necessary structural requirements.<sup>7</sup> We designed specific host molecules which would self-assemble via hydrogen bonds establishing a crystalline lattice commensurate with the repeat distance of the desired polymer. The host molecules would then bind to the guest monomers imposing upon them the proper spacing and orientation necessary for the polymerization (Figure 1). Using this methodology we have prepared in single crystal form several new polydiacetylenes, including the first examples of a terminal polydiacetylene<sup>8</sup> and poly(diiododiacetylene).<sup>9</sup> A similar host-guest approach led us to the first polytriacetylene<sup>10</sup> and the first polytriene<sup>11</sup> both via a SCSC polymerization as well.

There is considerable interest in the preparation of poly(aryldiacetylenes), polymers of diacetylenes with aryl groups directly attached to the acetylene carbon atoms.<sup>12</sup> Extending the conjugation of the polymer backbone on to the aromatic side groups may significantly enhance the electronic and optical properties of the modified PDAs. There have been many reported attempts to bring about a SCSC polymerization of an aryldiacetylene.<sup>13</sup> We have also tried to prepare a crystalline poly(aryldiacetylene), but have not been successful. Our best result was obtained by cocrystallizing 4,4'-dipyridyldiacetylene, with the oxalamide of glycine, **H<sub>2</sub>og**, as the host (Figure 3a).<sup>14</sup> The cocrystals exhibit very good structural parameters, but the

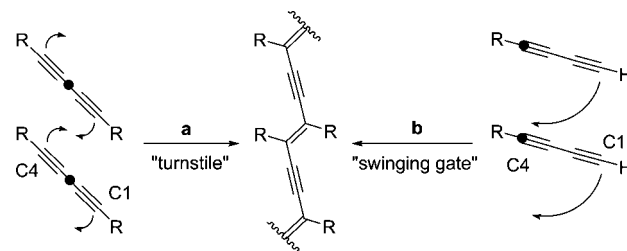


**Figure 2.** Two possible mechanisms for the topochemical polymerization of a diacetylene. (a) Turnstile mechanism. (b) Swinging gate mechanism.

polymerization does not go SCSC. Instead, the monomer crystals crumble into a purple powder as the polymerization progresses.

Similar frustrations have been reported by others for different aryldiacetylene derivatives, sometimes with monomer structures arranged in a perfect manner. Lee et al.<sup>15</sup> investigated the thermal polymerization of a bisbithazolyl diacetylene. Although the packing pattern in this work turned out to be excellent, with a 3.48 Å C1-C4 contact, the monomer crystals showed no polymerization at all in the solid state.

In an early study, Day and Lando<sup>16</sup> polymerized a cyclic bisphenyldiacetylene to an extent of 35% as confirmed by X-ray single crystal diffraction. In their work, the diacetylene moiety seems to follow the "turnstile" pathway (Figure 2) and the aromatic ring rotates by 19° about its axis. Nakanishi and co-workers<sup>17</sup> studied the solid state polymerization of a different bisphenyldiacetylene and was able to obtain polymerization of about 20%. In this case, the authors noticed a swinging motion of the phenyl ring associated with the polymerization. A complete topochemical SCSC polymerization was claimed for 1-(*N*-carbazolyl)-penta-1,3-diyne-5-ol, but no crystallographic analysis of the resulting polymer was reported.<sup>18</sup>

In most SCSC polymerizations the structural changes follow a reaction pathway corresponding to the turnstile mechanism.<sup>8,19,20</sup> As illustrated in Figure 2, when energy is applied the monomers pivot around their centers of mass in a conrotatory manner bringing the neighboring C1 and C4 carbon atoms together to form a new bond. The required atom movement is just over 1 Å for each reacting atom. This turnstile pathway is particularly favored for symmetrical diacetylenes.

The difficulties in SCSC polymerization of aryldiacetylenes may be attributed to the rigidity of aromatic pedant groups. When the polymerization occurs, the diacetylene functionality pivots like a "turnstile" by about 30° bringing the neighboring C1 and C4 carbon atoms together. The linear *sp* hybridized

- (7) (a) Fowler, F. W.; Lauher, J. W. *J. Phys. Org. Chem.* **2000**, *13*, 850–857. (b) Lauher, J. W.; Fowler, F. W.; Goroff, N. S. *Acc. Chem. Res.* **2008**, *41*, 1215–1229.
- (8) Xi, O. Y.; Fowler, F. W.; Lauher, J. W. *J. Am. Chem. Soc.* **2003**, *125*, 12400–12401.
- (9) Sun, A. W.; Lauher, J. W.; Goroff, N. S. *Science* **2006**, *312*, 1030–1034.
- (10) Xiao, J.; Yang, M.; Lauher, J. W.; Fowler, F. W. *Angew. Chem., Int. Ed.* **2000**, *39*, 2132–2135.
- (11) Hoang, T.; Lauher, J. W.; Fowler, F. W. *J. Am. Chem. Soc.* **2002**, *124*, 10656–10657.
- (12) (a) Sarkar, A.; Okada, S.; Matsuzawa, H.; Matsuda, H.; Nakanishi, H. *J. Mater. Chem.* **2000**, *10*, 819–828. (b) Chan, Y. H.; Lin, J. T.; Chen, I. W. P.; Chen, C. H. *J. Phys. Chem. B* **2005**, *109*, 19161–19168.
- (13) Recent examples include: (a) Blanchette, H. S.; Brand, S. C.; Naruse, H.; Weakley, T. J. R.; Haley, M. M. *Tetrahedron* **2000**, *56*, 9581–9588. (b) Sarkar, A.; Haley, M. M. *Chem. Commun.* **2000**, 1733–1734. (c) Rodriguez, J. G.; Lafuente, A.; Martin-Villamil, R.; Martinez-Alcazar, M. P. *J. Phys. Org. Chem.* **2001**, *14*, 859–868. (d) Nishinaga, T.; Nodera, N.; Miyata, Y.; Komatsu, K. *J. Org. Chem.* **2002**, *67*, 6091–6096. (e) Matsuo, H.; Okada, S.; Nakanishi, H.; Matsuda, H.; Takaragi, S. *Polym. J.* **2002**, *34*, 825–834. (f) Crihfield, A.; Hartwell, J.; Phelps, D.; Walsh, R. B.; Harris, J. L.; Payne, J. F.; Pennington, W. T.; Hanks, T. W. *Cryst. Growth Des.* **2003**, *3*, 313–320. (g) Rodriguez, J. G.; Lafuente, A.; De Los Rios, C. *J. Polym. Sci., Part A: Polym. Chem.* **2004**, *42*, 6031–6040. (h) Padgett, C. W.; Arman, H. D.; Pennington, W. T. *Cryst. Growth Des.* **2007**, *7*, 367–372.
- (14) Curtis, S. M.; Le, N.; Fowler, F. W.; Lauher, J. W. *Cryst. Growth Des.* **2005**, *5*, 2313–2321.

- (15) Lee, J. H.; Curtis, M. D.; Kampf, J. W. *Macromolecules* **2000**, *33*, 2136–2144.
- (16) Day, D.; Lando, J. B. *J. Polym. Sci., Part B: Polym. Phys.* **1978**, *16*, 1009–1022.
- (17) Nakanishi, H.; Matsuda, H.; Kato, M.; Theocharis, C. R.; Jones, W. *J. Chem. Soc., Perkin Trans. 2* **1986**, 1965–1967.
- (18) Matsuda, H.; Nakanishi, H.; Hosomi, T.; Kato, M. *Macromolecules* **1988**, *21*, 1238–1240.
- (19) Kane, J. J.; Liao, R. F.; Lauher, J. W.; Fowler, F. W. *J. Am. Chem. Soc.* **1995**, *117*, 12003–12004.
- (20) (a) Wilson, R. B.; Duesler, E. N.; Curtin, D. Y.; Paul, I. C.; Baughman, R. H.; Preziosi, A. F. *J. Am. Chem. Soc.* **1982**, *104*, 509–516. (b) Brouty, C.; Spinat, P.; Whuler, A. *Acta Crystallogr., Sect. C: Cryst. Struct. Commun.* **1984**, *40*, 1619–1624. (c) Aime, J. P.; Schott, M.; Bertault, M.; Toupet, L. *Acta Crystallogr., Sect. B: Struct. Sci.* **1988**, *44*, 617–624. (d) Foley, J. L.; Li, L.; Sandman, D. J.; Vela, M. J.; Foxman, B. M.; Albro, R.; Eckhardt, C. *J. Am. Chem. Soc.* **1999**, *121*, 7262–7263. (e) Irgartinger, H.; Skipinski, M. *Tetrahedron* **2000**, *56*, 6781–6794. (f) Xu, R.; Gramlich, V.; Frauenrath, H. *J. Am. Chem. Soc.* **2006**, *128*, 5541–5547.

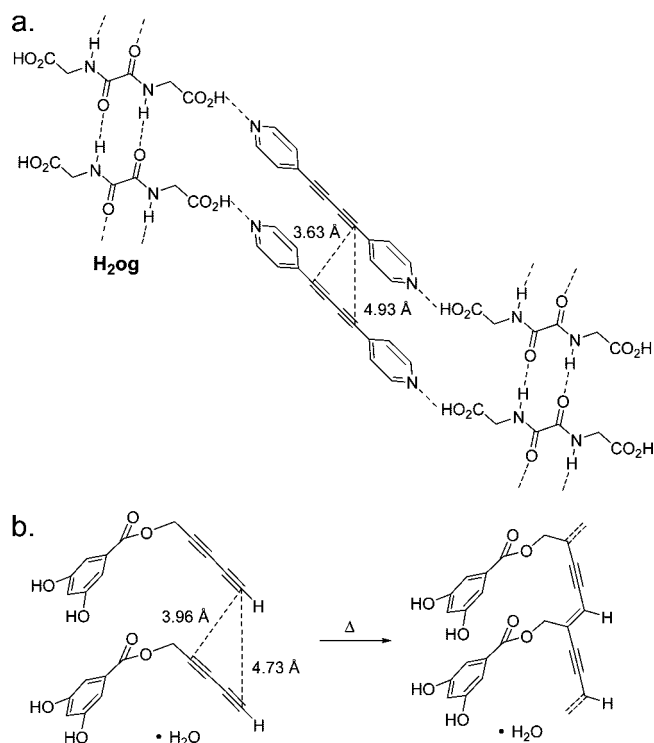


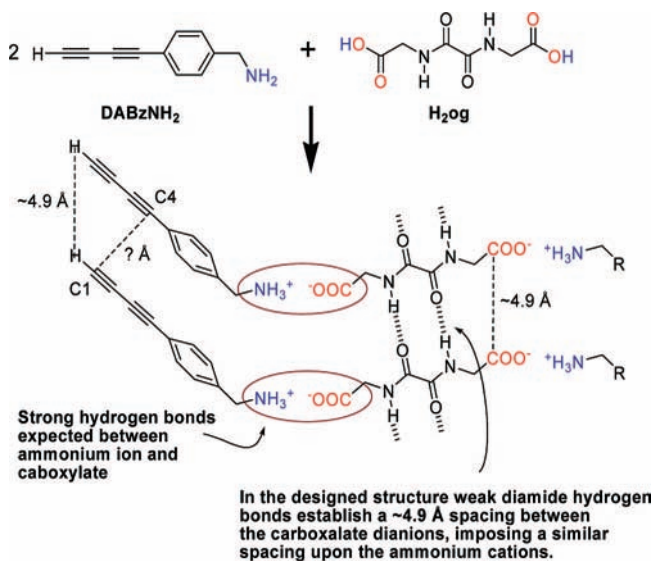
**Figure 3.** Two previously determined structures. (a) Structure of the cocrystal formed from 4,4'-dipyridyldiacetylene and the oxalamide of glycine,  $H_2og$ . In this designed structure, the oxalamide amide hydrogen bonds form a one-dimensional  $\alpha$ -network establishing the necessary intermolecular spacing in accordance with the parameters shown in Figure 1. (b) Structure of the hydrate crystal of a terminal diacetylene with resorcinol headgroup.

carbon atoms become trigonal centers with bond angles of  $120^\circ$ . The total angle change is  $60^\circ$  so the other half of the movement, another  $30^\circ$ , must involve the aromatic ring. This  $30^\circ$  movement of the rigid ring may just be too disruptive for the crystal lattice to remain intact. Both Lando's and Nakanishi's results support this speculation by the low percentage of polymerization and the movement of phenyl rings during the reaction in the crystalline state.

A mono substituted or terminal aryldiacetylene may be a solution. In a previous study<sup>8</sup> we found a reaction trajectory very different from the common "turnstile" mechanism, suggesting that perhaps an unsymmetrical aryldiacetylene can provide an alternate route to the preparation of poly(aryldiacetylene) single crystals. The inspiration came from a single crystal of penta-2,4-diynyl 3,5-dihydroxybenzoate monohydrate, which undergoes a facile SCSC polymerization with only moderate heating (Figure 3b). The surprising feature of this polymerization is the unsymmetrical reaction trajectory. A dramatic movement of  $2.5 \text{ \AA}$  by the terminal C1 carbon is the major contribution to the overall structural adjustment; in contrast C4 and its attached  $CH_2$  group only move slightly as the reaction proceeds. Thereby we proposed an idealized "swinging gate" mechanism, in which the C4 serves as a pivot point and all the movement required for new bond generation would take place at the terminal end of the diacetylene functionality (Figure 2b). This same mechanism could work just as well for a terminal aryldiacetylene, offering us a chance to achieve the long-standing goal of a SCSC aryldiacetylene polymerization.

Herein, we report the first poly(aryldiacetylene) single crystal to date, successfully prepared from the organic salt formed from a dicarboxylic acid host and a terminal aryldiacetylene guest.

**Scheme 1.** Supramolecular Design for a Host–Guest Salt Chosen to Achieve the Necessary Structural Parameters for a Topochemical Polymerization



Both the monomer and polymer structures are confirmed by X-ray single crystal diffraction along with other spectroscopic means of characterization. This study also sheds light on the supramolecular chemistry of organic salts, as an extension to the more common cocrystal approach to crystal engineering.

## Results and Discussion

When we first considered terminal aryldiacetylenes as potential polymerization targets, we initially chose 4-pyridyldiacetylene, the most straightforward target related to the previously studied 4,4'-dipyridyldiacetylene. Unfortunately, no quality cocrystals could be obtained, probably due to the extreme instability of the compound in the condensed state as often seen for terminal aryldiacetylenes.<sup>21</sup> Searching for an aryldiacetylene derivative with a substituent capable of forming hydrogen bonds to the standard host  $H_2og$ , we finally chose  $DABzNH_2$  as the targeted aryldiacetylene (Scheme 1).

Before proceeding with the nontrivial synthesis of  $DABzNH_2$ , we had an important question to consider. Could we realistically expect to successfully cocrystallize primary amine  $DABzNH_2$  with dicarboxylic acid  $H_2og$  to give a crystalline solid as outlined in Scheme 1? This would be an extension of previous studies where we relied on carboxylic acid to pyridine hydrogen bonds to provide us a greater variety of cocrystalline materials. However, potentially there was a big problem: a pyridine and a carboxylic acid will form a cocrystal; an amine like  $DABzNH_2$  should form a salt.

A pyridine-carboxylic acid cocrystal features one strong highly directional hydrogen bond; the structure of the complex can be predicted with confidence. An ammonium carboxylate salt will have a cation with three donor hydrogen atoms pointing in different directions and a carboxylate anion capable of accepting multiple hydrogen bonds from almost any angle. Thus there will be multiple strong, but nondirectional hydrogen bonds; a prediction of structure will be much more difficult.

**Salts.** The comparison of a cocrystal and a salt is not just a matter of semantics. If a carboxylic acid hydrogen bonds to a

(21) West, K.; Wang, C. S.; Batsanov, A. S.; Bryce, M. R. *J. Org. Chem.* **2006**, *71*, 8541–8544.

pyridine, there is no formal charge transfer and no ion formation. A typical substituted pyridinium ion has a  $pK_a$  of about 6, less acidic than a typical carboxylic acid  $pK_a$  of about 4.5, but not by much.<sup>22</sup> In solution a carboxylic acid will protonate a pyridine, but in the solid state in the absence of stabilizing solvent molecules there usually is no proton transfer and a carboxylic acid will simply form a hydrogen bond with a pyridine.

The situation with a substituted benzylamine is different. A substituted benzylammonium ion has a  $pK_a$  of about 9.5, considerably less acidic than a carboxylic acid.<sup>22</sup> Proton transfer is expected in the solid state and an ammonium carboxylate salt will form instead of a cocrystal. The resulting primary ammonium and carboxylate anion will form strong hydrogen bonds and will likely dominate the molecular packing in the salt crystals. Indeed one can refer to these strong interactions as “coulomb or ionic interactions” as opposed to normal hydrogen bonds, but since all such forces lie on a continuum of energy we find it convenient to simply call them “strong hydrogen bonds.” It was not at all clear that the necessary one-dimensional  $\alpha$ -network based upon weaker amide-amide hydrogen bonds between host molecules will form in the presence of these strong hydrogen bonds.

A recent paper by Aakeroy et al.<sup>23</sup> focuses on this problem. They prepared and compared 61 different cocrystals with 21 different organic salts. The series of cocrystals gave crystals with predicted stoichiometries 95% of the time, but 45% of the salts gave alternate stoichiometries or incorporated solvent. We were thus somewhat apprehensive that the structure of Scheme 1 might not form. Therefore before proceeding with the synthesis of our target compound **DABzNH<sub>2</sub>**, we prepared a test series of ten different salts of our host dicarboxylic acid **H<sub>2</sub>og**.

**Model Studies.** Our test series started with the ammonium ion, included the simple alkyl ammonium ions from methyl through hexyl, plus three cyclic ammonium ions, derived from cyclohexyl, benzyl and 4-ethynylbenzyl amines. The salts were all prepared by adding two equivalents of each amine to a small quantity of dicarboxylic acid **H<sub>2</sub>og** in water or water/methanol solutions. In each case crystals formed upon slow evaporation at a temperature of  $\sim 35$  °C. Once a first crystal structure was obtained from each of the test cases, no further investigations were made. No attempt was made to find a second polymorph or solvate of any of the model compounds. Our initial results confirmed the observations of Aakeroy. The simplest salts all failed to give the supramolecular structures necessary for topochemical polymerizations. Indeed we seemed to have undertaken a study of chaos.

**Ammonium Salt.** This first case illustrates the problem. One characteristic of dicarboxylic acids is that quite often their half-neutralized salts will readily crystallize from solution, usually yielding excellent crystals. Crystals of most half-neutralized dicarboxylic acids contain a strong hydrogen bond between the remaining carboxylic acid hydrogen and the single carboxylate. A common example is potassium hydrogen tartrate, a well-known crystalline byproduct of wine making.<sup>24</sup> A search of the Cambridge Structural Database (CSD)<sup>25</sup> yields a raw count of 204 structures containing the hydrogen tartrate ion, but only 147 structures containing the tartrate dianion. Hydrates are also

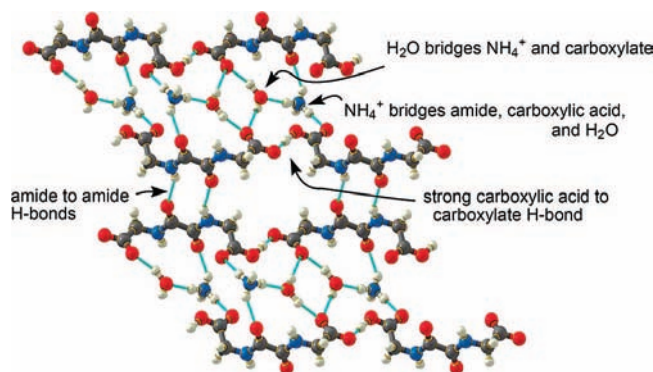


Figure 4. Crystal structure of  $\text{NH}_4\text{Hog} \cdot 2\text{H}_2\text{O}$ .

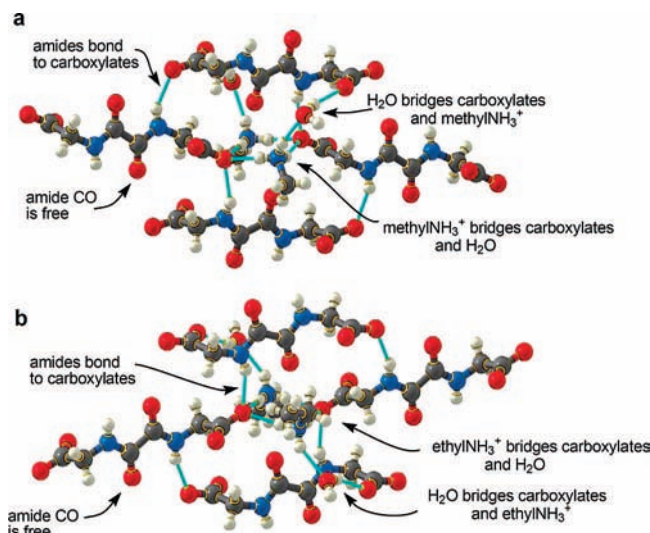


Figure 5. Crystal structures of (a)  $(\text{methylNH}_3)_2\text{og} \cdot 2\text{H}_2\text{O}$  and (b)  $(\text{ethylNH}_3)_2\text{og} \cdot 2\text{H}_2\text{O}$ .

common; 75 of the hydrogen tartrate structures and 109 of the tartrates are hydrates.

Thus we are not surprised to find that **H<sub>2</sub>og** crystallizes from aqueous ammonia to give the hydrated half-neutralized salt  $\text{NH}_4\text{Hog} \cdot 2\text{H}_2\text{O}$  (Figure 4). The  $\text{Hog}^{-1}$  ions form a chain via the strong carboxylic acid to carboxylate hydrogen bond. One set of amide-amide hydrogen bonds forms, but the linear  $\alpha$ -network of amide hydrogen bonds shown in Scheme 1 is not found. Instead the second amide oxygen atom forms a hydrogen bond to an ammonium ion.

**Methyl- and Ethylammonium Salts.** Methyl- and ethylamine form similar salts with **H<sub>2</sub>og**. The supramolecular chemistries of the two salts are the same, but the crystallographic symmetries are different (Figure 5). In each case the dicarboxylic acid host is fully neutralized to form a dicarboxylate anion. The ammonium ions bridge a water molecule plus two carboxylates end to end. The amide hydrogen atom forms a hydrogen bond to a carboxylate as well. The required supramolecular structural features of Scheme 1 do not exist.

**Propylammonium Salt.** With propylamine, a fully neutralized anhydrous salt forms. The oxalamide  $\alpha$ -network is seen for the first time, but with two molecules per asymmetric unit, not one

(22) Albert, A.; Serjeant, E. P. *The Determination of Ionization Constants*; Chapman and Hall: London, 1984.

(23) Aakeroy, C. B.; Fasulo, M. E.; Desper, J. *Mol. Pharmacol.* **2007**, *4*, 317–322.

(24) Kroon, J.; Kanters, J. A. *Acta Crystallogr., Sect. B: Struct. Sci.* **1972**, *B 28*, 714–722.

(25) Allen, F. H. *Acta Crystallogr., Sect. B: Struct. Sci.* **2002**, *58*, 380–388.

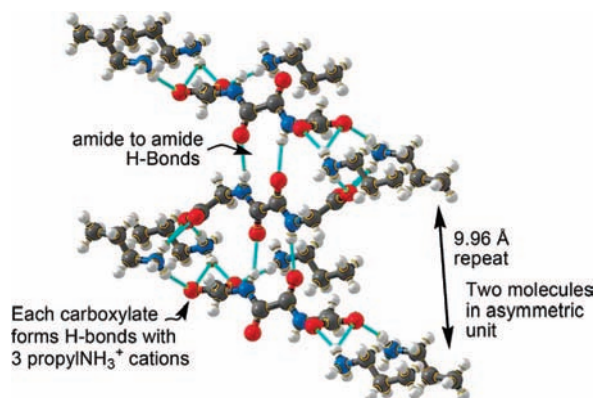


Figure 6. Crystal structure of  $(\text{propylNH}_3)_2\text{og}$ .

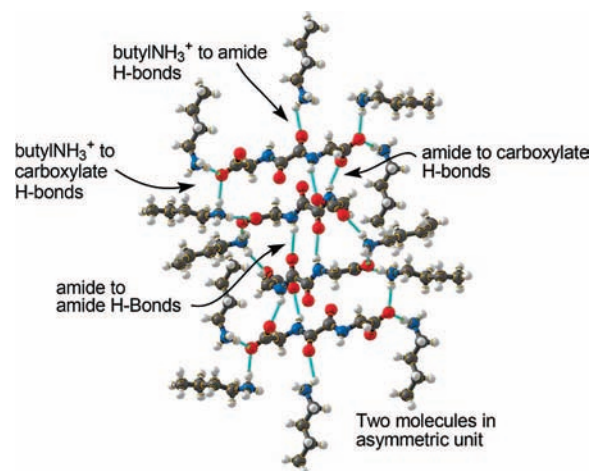


Figure 7. Crystal structure of  $(\text{butylNH}_3)_2\text{og}$ .

(Figure 6). This means the crystallographic repeat unit is doubled to  $\sim 10$  Å instead of the necessary 4.9 Å. The propyl ammonium ions form a full set of hydrogen bonds to the carboxylates, but, because of the multiple molecules in the asymmetric unit, the structure parameters do not correspond to those needed for a diacetylene polymerization.

**Butylammonium Salt.** The salt with butylamine,  $(\text{butylNH}_3)_2\text{og}$ , was not at all encouraging. There are two molecules in the asymmetric unit and seemingly no pattern to the hydrogen bonds (Figure 7). One pair of molecules forms a diamide dimer, but the other molecule in the asymmetric unit formed only amide to carboxylate hydrogen bonds.

**Pentyl- and Hexylammonium Salts.** The results with pentyl- and hexylamine are much closer to the designed structure shown in Scheme 1 (Figure 8). The host molecules of both structures form a one-dimensional amide-amide hydrogen bond  $\alpha$ -network. Superficially the two structures look similar, but a closer look shows that their stoichiometries are different. The hexylamine structure is the simplest; it is the hexylammonium salt of the half-neutralized host,  $\text{Hog}^{-1}$ . The pentylamine structure has one fully neutralized  $\text{og}^{-2}$  dianion plus one fully protonated diacid molecule,  $\text{H}_2\text{og}$ . However, the important fact is that both structures exhibit the targeted 4.9 Å repeat distance established by the amide-amide hydrogen bonds. In each structure there is a segregation of the weak amide-amide hydrogen bonds from the stronger carboxylate-ammonium and carboxylate-carboxylic acid hydrogen bonds.

**Cyclic Primary Ammonium Salts.** The next logical step in our series of model salts was to examine cyclic primary amine

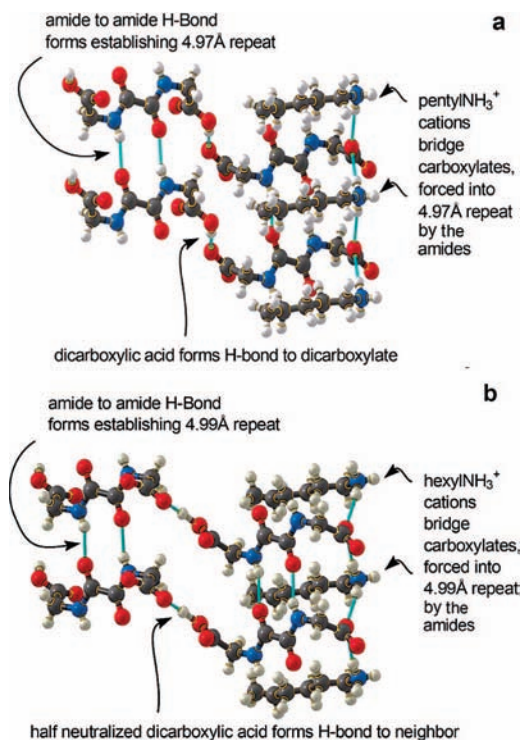


Figure 8. Crystal structures of (a)  $(\text{pentylNH}_3)_2\text{og} \cdot \text{H}_2\text{og}$  and (b)  $(\text{hexylNH}_3)_2\text{Hog}$ .

salts. Cyclohexyl- and benzylamine formed simple fully neutralized salts, of the form  $(\text{RNH}_3)_2\text{og}$ . Each crystallized in the triclinic  $P\bar{1}$  space group with one formula unit per unit cell. Each formed a two-dimensional  $\beta$ -network of  $p\bar{1}$  layer group symmetry exhibiting the supramolecular chemistry projected in Scheme 1. These layers are pictured in Figure 9 along with a sketch of the two-dimensional layer unit-cells. There are two independent hydrogen bond  $\alpha$ -networks along the short ( $\sim 5$  Å) unit cell direction (Figure 10). The first is the oxalamide  $\alpha$ -network, previously shown to be a reliable functionality for establishing a 4.9–5.0 Å spacing. Parallel to the oxalamide  $\alpha$ -network is an  $\alpha$ -network of alternating pairs of primary ammonium cations and carboxylate anions.

This primary ammonium carboxylate network has been seen before, but it is not common. Sada and co-workers<sup>26</sup> recently published a comprehensive CSD analysis of ammonium carboxylate structures. They identified 1070 examples of primary alkyl ammonium carboxylate salts. These salts formed a wide variety of one and two-dimensional hydrogen bonded networks. Only 47, less than five percent of the structures formed the one-dimensional  $\alpha$ -network shown in Figure 10b. These 47 structures were not identified specifically and we have not reproduced their extensive study ourselves, but a more casual perusal of the CSD indicates that this network is found in structures of various racemic  $\alpha$ -amino acids. Qualitatively the crystallographic repeat distances appear to range from about 4.6 to 4.9 Å, generally shorter than the distance targeted and found in the salt system studied here. A typical example is the racemic phenylglycine which contains the  $\alpha$ -network of Figure 10b with a repeat distance of 4.85 Å.<sup>27</sup>

These model studies gave us a strong indication that the design of Scheme 1 would work, thus we proceeded with the

(26) Sada, K.; Tani, T.; Shinkai, S. *Synlett* **2006**, 2364–2374.

(27) Dalhus, B.; Görbitz, C. H. *Acta Crystallogr., Sect. C: Cryst. Struct. Commun.* **1999**, 55.

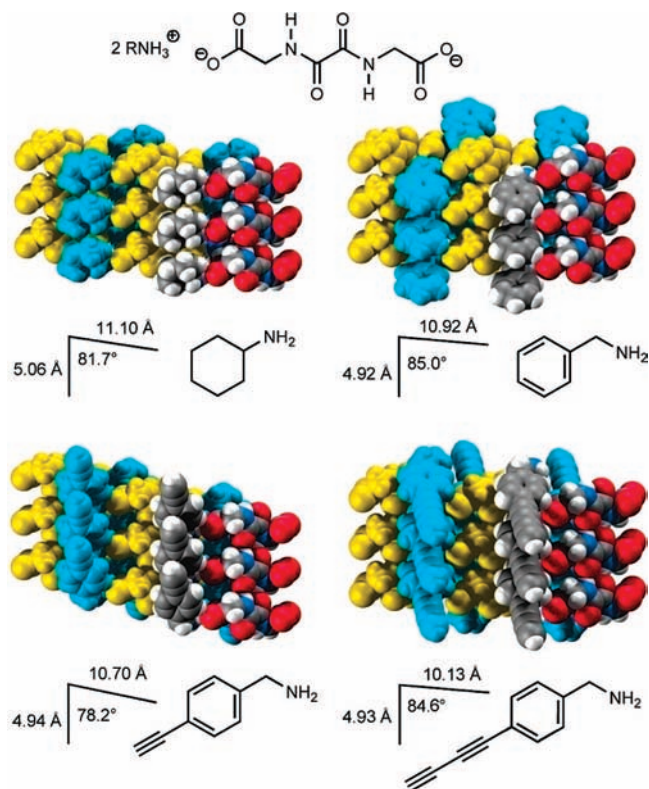


**Figure 9.** The crystal structures of four cyclic ammonium salts of the form  $(\text{RNH}_3)_2\text{og}$ . The supramolecular chemistries of the four  $\alpha$ -networks are identical. Each layer contains the two independent hydrogen bonding networks shown in Figure 10. The four layers each have  $p1$  layer group symmetry with two-dimensional unit cells of similar dimensions as indicated in the drawing.

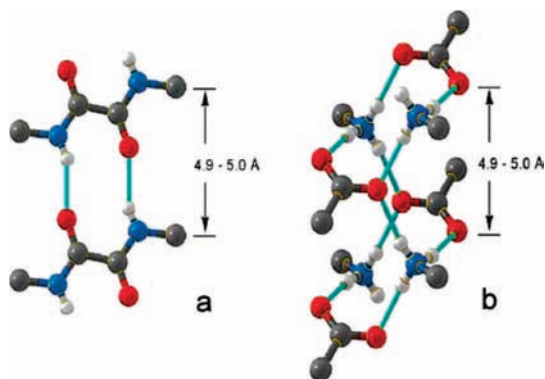


**Figure 10.** Two independent parallel  $\alpha$ -networks found within the  $\beta$ -networks of the cyclic ammonium salts shown in Figure 9. (a) Well-known oxalamide  $\alpha$ -network. (b) Not-so-commonly observed ammonium carboxylate  $\alpha$ -network.

synthesis of 4-diacetylenylbenzylamine ( $\text{DABzNH}_2$ ). As described later in this paper (Scheme 2), the monoacetylene compound 4-ethynylbenzylamine ( $\text{EBzNH}_2$ ) was a model compound from the synthesis. This gave us the opportunity for one more model in the crystallographic study. The amine  $\text{EBzNH}_2$  also formed a simple salt of the form,  $(\text{RNH}_3)_2\text{og}$ , with a layer structure analogous to the cyclohexyl- and benzylamine salts (Figure 9). The only difference in the structure was the orientation of the 4-ethynylbenzyl group, which can be seen to bend “up” opposite in direction to the benzyl group that bends “down.”

**Targeted 4-Diacetylenylbenzylamine Salt.** This brings us to the designed amine  $\text{DABzNH}_2$ . It also formed a simple salt of the form  $(\text{RNH}_3)_2\text{og}$  (Figure 9). The structure was a close analogue of the three cyclic primary amine salts studied as models. The all important diacetylene repeat distance was 4.93 Å and the neighboring C1–C4 distance was 3.57 Å. These parameters are well within the range needed for a topochemical polymerization.

As we examined the various model salts we made no attempt to search for polymorphs of alternate solvated crystals, but with diacetylene  $\text{DABzNH}_2$  an active search for alternate crystalline forms was not necessary. The partial polymerization of the diacetylene moiety introduces color into the crystals making it very easy to identify crystal variants. We found two alternate crystalline forms without really looking for them. The desired solvent free salt discussed above came out of mixed methanol/water solutions as pink needles, but the needles were accompanied by red plates of a hydrated crystalline form,  $(\text{DABzNH}_3)_2\text{og}\cdot 2\text{H}_2\text{O}$  (Figure 11).

The host anions in the hydrate do not align in accordance with the design of Scheme 1. However, the ammonium ions do form a water bridged network along a glide plane that brings neighboring diacetylenes into approximate alignment with a repeat distance of 9.53 Å for a pair of symmetry related molecules. Neighboring molecules have end–end distance of 4.81 Å and a C1–C4 distance was 3.52 Å, even shorter than the value of 3.57 Å found in the anhydrous crystal. Thus we had in hand two possible candidate structures for the topochemical polymerization, one designed and one accidental.

We also found a third crystalline form, a methanol solvate,  $(\text{DABzNH}_3)_2\text{og}\cdot 2\text{CH}_3\text{OH}$  (Figure 12). In this form the diacetylenic ammonium cations are well separated and there are no amide–amide hydrogen bonds. This form seems totally unsuitable for a topochemical polymerization.

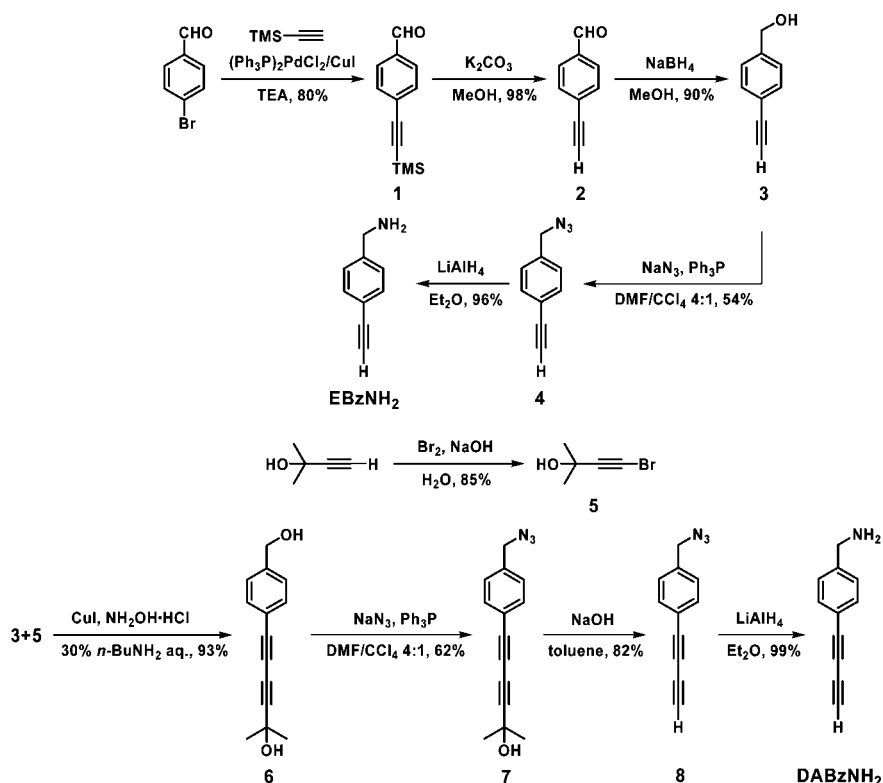
Once we understood that the  $\text{DABzNH}_2$  readily formed solvated crystals it became important to find a reliable way of growing the solvent free form exclusively. This could be done simply by using pure 1-propanol for the crystallization, although the efficiency of the supramolecular synthesis was limited by the poor solubility of  $\text{H}_2\text{og}$  in this solvent.

**Layered Salts.** The four cyclic primary ammonium salts form isostructural layers as shown in Figure 9. In Figure 13 a top view of these layers can be seen. The layers have the form of a reverse bilayer with the charged residues in the center of the layer and the nonpolar greasy tails pointing outward on both sides of the layer. Such layered organic salts have been seen before. Good examples include Zaworotko’s<sup>28</sup>  $N,N$ -dibenzylammonium carboxylate laminated clay mimics and Ward’s<sup>29</sup> guanidinium sulfonates. A common theme to these layered salts seems to be the need for a greasy group of sufficient size to drive the bilayer formation via forces similar to the hydrophobic effect. This is illustrated by the fact that the smaller ammonium cations in this study failed to form the layer structures formed by the larger and greasier ammonium cations (Table 1). The  $\pi$ - $\pi$  interactions may also play active roles if they exist, as they do in the cases of the benzyl-, 4-ethynylbenzyl- and the targeted 4-diacetylenylbenzyl ammonium salts.

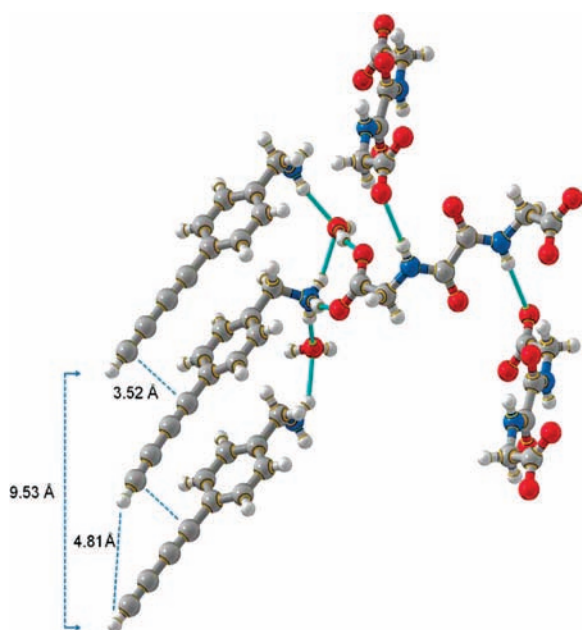
The  $p1$  layer group symmetry is constant for all four layers. The dimensions of the two-dimensional layer unit cells are

(28) Biradha, K.; Dennis, D.; MacKinnon, V. A.; Sharma, C. V. K.; Zaworotko, M. J. *J. Am. Chem. Soc.* **1998**, *120*, 11894–11903.

(29) Horner, M. J.; Holman, K. T.; Ward, M. D. *Angew. Chem., Int. Ed.* **2001**, *40*, 4045–4048.

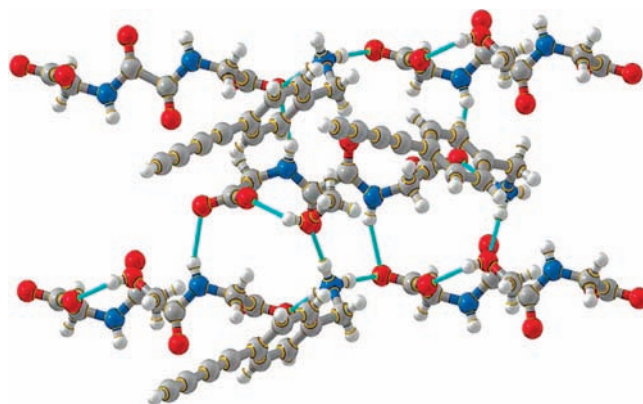
Scheme 2. Synthesis of EBzNH<sub>2</sub> and DABzNH<sub>2</sub>

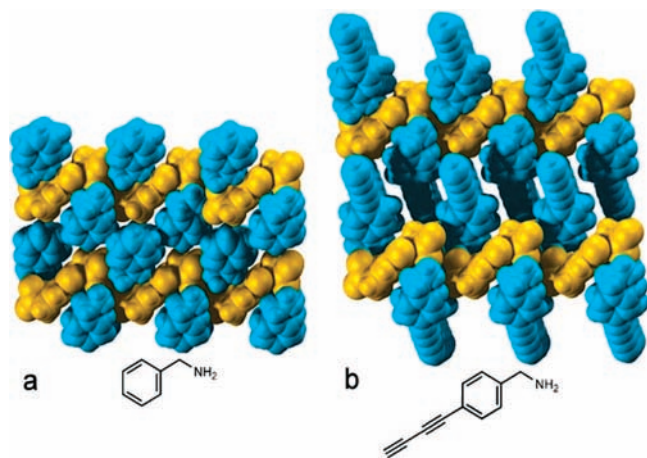
similar as diagrammed in Figure 9. Three of the layers, the 4-ethynylbenzylammonium salt being the exception, stack via simple translation to give a crystal with *P1* space group symmetry. The 4-ethynylbenzylammonium salt stacks via a *2*<sub>1</sub> screw axis to give a crystal with *P2*<sub>1</sub>/*n* space group symmetry. This is significant, because it shows how different supramolecular assemblies can vary at different levels of structure analysis. In this case the basic design of Scheme 1 was adopted by all four of the cyclic ammonium salts. They form isostructural layers with identical chemistry and identical crystallographic

Figure 11. Structure of the hydrate, (DABzNH<sub>3</sub>)<sub>2</sub>·og·2H<sub>2</sub>O.

symmetry. When the stacking of the layers is considered, three of the salts are still isostructural but the fourth is different. Fortunately, our design for a diacetylene polymerization only required two dimensions of control, not three.

**Synthesis.** The compounds EBzNH<sub>2</sub> and DABzNH<sub>2</sub> were prepared as outlined in Scheme 2. The synthesis of the two *para*-substituted benzylamines both started with 4-bromobenzaldehyde, after three successive steps of the Sonogashira coupling, removal of the silyl protecting group and reduction, alcohol **3** was prepared. This benzylalcohol was converted to an azide **4** in one step using Reddy's procedure,<sup>30</sup> followed by a reduction to yield EBzNH<sub>2</sub>. For the terminal diacetylene synthesis, another building block, bromide **5**, was attained from 2-methyl-3-butyl-2-ol. Then the Cadiot-Chodkiewicz coupling of **3** and **5** afforded the protected diacetylene **6**, which was directly converted to the azide **7**. After the elimination of acetone protecting group followed by a reduction of the azide group, the target compound

Figure 12. Structure of the methanol solvate, (DABzNH<sub>3</sub>)<sub>2</sub>·og·2CH<sub>3</sub>OH.



**Figure 13.** Top view of two of the layers shown in Figure 9. (a)  $(\text{benzylNH}_3)_2\text{og}$ . (b)  $(\text{DABzNH}_3)_2\text{og}$ . The layers form an inverse bilayer with the hydrophobic tails of the ammonium salts filling the space between the hydrogen bonded anions.

**Table 1.** Summary of the Structural Characteristics in  $(\text{RNH}_2)_x(\text{H}_2\text{og})_y$  Salts

R	stoichiometry (xy)	desired H-bond $\alpha$ -networks among hosts	repeat distance
H, $\text{CH}_3$ , ethyl <i>n</i> -propyl, <i>n</i> -butyl	1:1 or 2:1 ( <i>w</i> $\text{H}_2\text{O}$ )	Not found	—
<i>n</i> -pentyl	1:1	found	4.97 Å
<i>n</i> -hexyl	1:1	found	4.99 Å
cyclohexyl	2:1	found	5.06 Å
benzyl	2:1	found	4.92 Å
4-ethynylbenzyl	2:1	found	4.94 Å
4-diacetylnylbenzyl	2:1	found	4.93 Å

$\text{DABzNH}_2$  was obtained in an overall yield of 35%. As a terminal aryldiacetylene,  $\text{DABzNH}_2$  was found chemically unstable. It can be stored in solution at low temperature for months. However, once the stock solution is concentrated, this reactive amine turns quickly from white crystals into a deep-colored insoluble solid, as do most of the terminal aryldiacetylenes discussed in the literature.<sup>21</sup>  $\text{H}_2\text{og}$  was synthesized according to a procedure adapted from the literature.<sup>31</sup>

The high quality single crystals of  $\text{DABzNH}_2$  salt were difficult to grow. All three forms of  $\text{DABzNH}_2/\text{H}_2\text{og}$  salts were finally obtained by solvent evaporation of the stoichiometric quantities of host and guest in anhydrous alcohol or methanol/ $\text{H}_2\text{O}$  mixture at room temperature. The methanol solvate crystals were obtained when methanol was used; a mixture of the hydrate form and the solvent-free form was obtained when methanol/ $\text{H}_2\text{O}$  mixture was used; while the pure solvent-free form was obtained when anhydrous 1-propanol was used. It is crucial that the evaporation rate is much faster than normal, as the conditions used for the model salts take from overnight to a couple of days before the crystals appear. A rapid evaporation approach is very important when dealing with unstable compounds like  $\text{DABzNH}_2$  and can be realized using a wide open container like a Petri dish. It usually takes less than 30 min to get high quality single crystals of  $\text{DABzNH}_2/\text{H}_2\text{og}$  salts from about 10 mL solution. The regular slow evaporation never worked well

due to the problems presumably caused by the chemical instability of  $\text{DABzNH}_2$  in a concentrated state. Other standard techniques for crystal growth, such as cooling methods, vapor diffusion and solvent diffusion, have also been tested although none of them gave satisfactory results. The significant difference between the solubilities of  $\text{DABzNH}_2$  and  $\text{H}_2\text{og}$  complicates all of these alternate crystallization methods.

**Polymerization.** Once the crystallographic work was finished it was found that there were two candidate crystals for the SCSC polymerization study. The designed solvent free structure,  $(\text{DABzNH}_3)_2\text{og}$ , and the unexpected hydrate,  $(\text{DABzNH}_3)_2\text{og} \cdot 2\text{H}_2\text{O}$ .

The hydrate crystals formed as red plates suggesting that some degree of polymerization was taking place at room temperature. The crystal structure showed that the monomers were aligned along a glide plane with good structural parameters for a topochemical polymerization (Figure 10). Heating the crystals turned their color from the original red to a much darker essentially black color. Such color changes are usually indicative of further polymerization. The single crystal used for the original structure determination was heated in a controlled manner to 80 °C for 12 h. A visual examination of the crystal showed a darker color, but numerous cracks had developed and major portions of the crystal simply crumbled away. The crystal was returned to the diffractometer and reexamined. No further diffraction could be observed. Other crystals of the hydrate showed similar changes upon heating. It seems most likely that these changes are due to loss of water from the crystal lattice. Since the anhydrous crystals were giving us better results we abandoned our studies of the hydrate.

The crystal structure of the anhydrous crystals,  $(\text{DABzNH}_3)_2\text{og}$ , revealed a near perfect packing of the diacetylene monomers. The crystallographic repeat distance of 4.93 Å is very close to the targeted 4.9 Å spacing. The C1–C4 contact distance between neighboring monomers was 3.57 Å, well set up for an intramolecular reaction. With such promising structural parameters we anticipated that the polymerization would occur readily. In previous work with a terminal diacetylene, the hydrated compound shown in Figure 3b, polymerization took place at a temperature of only 50 °C despite the fact that structural parameters were seemingly less satisfactory than those found in this structure. Initial experiments showed us that the  $(\text{DABzNH}_3)_2\text{og}$  crystals turned dark at temperatures well above 100 °C. For example a crystal heated at 150 °C for 16 h appeared to be polymerized, but unfortunately diffraction studies indicated an amorphous structure. The polymerization was further confirmed by DSC analysis (Figure S7, Supporting Information), FT-IR (Figure S9, Supporting Information) and Raman spectroscopy (Figure S10, Supporting Information), but the goal of our work was a SCSC polymerization. This was achieved by a carefully controlled series of annealing experiments.

**Single-Crystal-to-Single-Crystal Polymerization Study.** Several different crystalline samples were examined, but this report will focus on the structural results for one single crystal study that was carried out over a period of about three months. Initial experiments with other crystals indicated that a slow polymerization was the only way that we could maintain the crystal integrity of the sample.

The monomer crystal selected had a pale pink color. It was glued to a glass fiber for the X-ray experiment and a structure determination was carried out. The refinement was normal and there was no sign of polymerization. The initial monomer structure is shown in Figures 14 and 15. This single crystal was then placed in a

(30) Reddy, G. V. S.; Rao, G. V.; Subramanyam, R. V. K.; Iyengar, D. S. *Synth. Commun.* **2000**, *30*, 2233–2237.

(31) Hearn, W. R.; Hendry, R. A. *J. Am. Chem. Soc.* **1957**, *79*, 5213–5217.



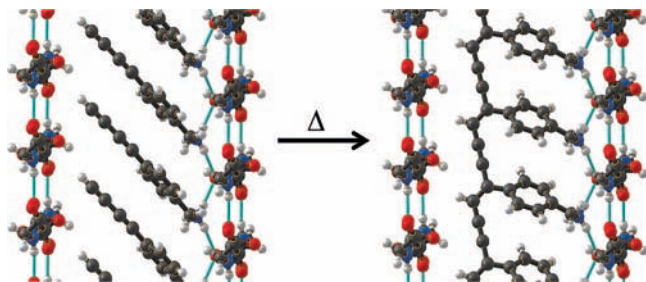


**Figure 14.** On the left is a view of the crystal structure of the  $(\text{DABzNH}_3)\text{og}$  salt. The right-hand side shows a similar view of the polymerized structure. The same crystal was used for both experiments.

vacuum oven at 100 °C for a day, the crystal was observed to be darker in color and its structure was redetermined. The structure was refined and a new set of peaks appeared in the electron density maps. These peaks corresponded to the emerging polymer and had an occupancy of 11%. As shown in Table 2, additional heat treatments at 100 °C were carried out over a period of a month. The occupancies of the atoms corresponding to the polymer reached 45%. The temperature was then raised for subsequent experiments. After 66 days of heating, with a final temperature of 145 °C the polymerization was observed to be 78% meaning that the polymer atoms were now the major atoms present and the monomer atoms made up the minor set. At this point the temperature was increased to 160 °C to speed up the transition. Unfortunately, the crystal no longer gave a useful diffraction pattern. Raman spectrum of such fully annealed crystals gave no definitive evidence of the monomer and the final polymerization seems to be essentially 100%.

The polymer structure shown in Figure 14 and Figure 15 is the result obtained from the 78% structure, corresponding to experiment entry 12 in Table 2. An examination of the crystallographic parameters shows that the unit cell steadily contracts along the short *a*-axis as the polymerization proceeds from 4.93 to 4.89 Å. The *a*-axis corresponds to the orientation of the polymer backbone. The overall volume change leads to a two percent decrease in the crystal density.

As discussed in the introduction we chose to study an terminal aryldiacetylene working on the assumption that the major movement during the polymerization would involve the hydrogen end of the diacetylene and the phenyl end would not need to move much or at all. An examination illustrated in Figure 15 shows that the opposite has occurred. The terminal C1 carbon has moved the least, 1.7 Å, while C4 next to the phenyl ring has moved the most, 3.0 Å, a very large movement when compared to previous topochemical polymerizations. The entire phenyl group has pivoted on its axis roughly along the C8–C9 bond and moved “downward” and to the side following the C4 atom. A similar phenomenon has been noticed in the Nakanishi’s work, where the authors achieved only a 20% conversion to polymer in their bisphenyldiacetylene crystals.<sup>17</sup>

In the monomer structure the phenyl ring has a dihedral angle of 89.9° with respect to the short crystallographic axis of 4.93 Å. In the polymer the phenyl pivot has brought this dihedral angle down to 38.7°. This is essentially as small as this dihedral angle can go since the nonbonded contacts between atoms of neighboring phenyl rings are in van der Waals contact of 3.3 Å (Figure 16).

## Conclusion

We set as our goal, the design and realization of a single-crystal-to-single-crystal polymerization of a terminal aryldi-

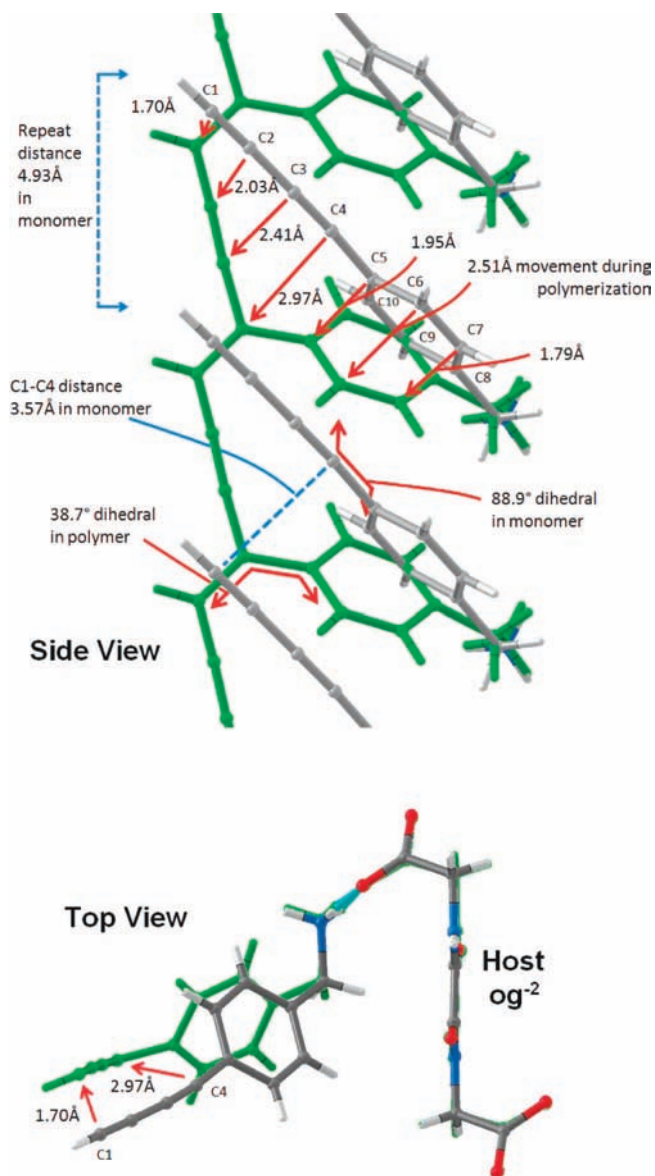


**Figure 15.** Detailed structural analysis of the monomeric and polymeric forms of  $(\text{DABzNH}_3)_2\text{og}$ . The monomer atoms are colored normally; the polymer is in all green.<sup>32</sup> The top of the figure shows a side view of the monomers and the corresponding polymer. The bottom of the figure shows a top view of the same structure and includes the host molecule. The host molecule changes little during the polymerization reaction. The monomers move downward bending at the middle C4 carbon. There is also a sideways movement as seen in the top view. Carbon C4 moves the most, 2.97 Å. The initial monomer spacing of 4.93 Å is very close to the ideal value. The corresponding polymer value is slightly shorter at 4.89 Å. Upon polymerization the phenyl ring turns on its axis by about 50°.

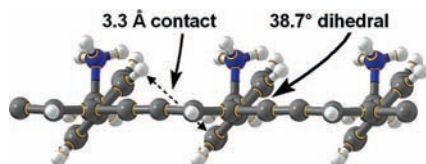
acetylene. This goal was achieved and along the way we have learned some lessons that should be useful in future supramolecular syntheses.

For many years we have relied upon cocrystallization as the basis of our host–guest strategy. This was our first attempt to use an anion host to organize a cationic guest. An examination of the literature told us this might be difficult. Consistent with this pessimistic view model compounds with small cations followed no general pattern, but larger and “greasier” cations worked just fine. There appeared to be a hydrophobic like dominated segregation that separated the highly charged salt functionalities from the rest of the structure. This segregation allowed the amide–amide hydrogen bonds to form in the normal

**Table 2.** Single Crystal Annealing History and Resulting Unit Cell Constants

	heating temp. (° C)	heating interval (days)	cumulative time (days)	a (Å)	b (Å)	c (Å)	$\alpha$ (deg)	$\beta$ (deg)	$\gamma$ (deg)	volume (Å <sup>3</sup> )	percent polymer <sup>c</sup>
<b>1<sup>a</sup></b>	—	—	—	4.931(3)	10.017(7)	13.738(9)	85.899(14)	84.56(2)	85.141(16)	671.7(8)	0
<b>2</b>	100	1	1	4.913(2)	10.032(3)	13.752(4)	85.437(6)	84.967(7)	85.201(6)	671.0(4)	11
<b>3</b>	100	2	3	4.908(1)	10.029(3)	13.741(4)	85.123(7)	85.141(6)	85.225(5)	669.5(3)	14
<b>4</b>	100	3	6	4.914(1)	10.048(2)	13.754(3)	84.784(6)	85.293(4)	85.220(6)	672.1(3)	25
<b>5</b>	100	4	10	4.909(2)	10.046(4)	13.738(5)	84.172(7)	85.592(6)	85.255(7)	670.1(4)	30
<b>6</b>	100	7	17	4.912(2)	10.061(5)	13.740(6)	83.478(7)	85.857(10)	85.221(8)	671.0(5)	34
<b>7</b>	100	7	24	4.917(3)	10.075(7)	13.744(9)	82.745(8)	86.223(13)	85.270(10)	672.1(7)	38
<b>8</b>	100	7	31	4.910(2)	10.066(4)	13.723(5)	82.422(6)	86.377(8)	85.273(7)	669.1(5)	45
<b>9</b>	120	7	38	4.901(1)	10.071(3)	13.693(4)	81.027(5)	87.160(8)	85.367(7)	665.0(3)	50
<b>10</b>	130	7	45	4.899(1)	10.075(3)	13.680(4)	80.483(6)	87.538(5)	85.453(6)	663.5(3)	55
<b>11</b>	130	7	52	4.899(2)	10.083(3)	13.690(4)	79.831(7)	88.034(6)	85.553(7)	663.4(3)	57
<b>12</b>	145	14	66	4.886(2)	10.072(4)	13.670(5)	79.154(6)	88.615(9)	85.662(8)	658.8(4)	78
<b>13<sup>b</sup></b>	160	17	83	—	—	—	—	—	—	—	—

<sup>a</sup> Experiment 1 gives the cell constants of the monomer crystal before any heat treatment. <sup>b</sup> Experiment 13 destroyed the crystal integrity; no unit cell could be obtained. <sup>c</sup> Percentage of polymerization is a qualitative estimate based upon fractional atom occupations in the least squares refinement.

**Figure 16.** Illustration of the relative positions of neighboring phenyl rings along the backbone in the polymer crystals.

manner establishing the required spacing for the designed diacetylene polymerization.

Previous reports on disubstituted aryldiacetylenes all failed to produce single-crystal-to-single-crystal polymerizations. This was likely due to the major disruption caused by required movement of the aryl groups. It was our hypothesis that a terminal aryldiacetylene would require less movement of the aryl group. Surprisingly our design worked, but the single aryl group still undergoes a major movement in the solid state. The phenyl groups pivot by about 50° as the reaction proceeds. The major driving force for this movement seems to be the need for neighboring phenyls to maintain their van der Waals contact, Figure 16. The polymerization reaction trajectory is closer to that of the “swinging gate” than the “turnstile”, Figure 2, but the “gate” is swinging in a manner we did not anticipate.

(32) The two structures were superimposed by using closest carbonyl carbon atom of the nearest oxalamide host molecule to establish a common origin. The z axis of a common orthogonal coordinate system was defined by the shorta axes of the two superimposed unit cells. The plane of the two central carbonyl groups was used to establish the xz coordinate plane; the y axis was normal to this plane.

An important aspect of this study is the slow annealing of the single crystal used in the X-ray diffraction study. A three month long series of slow heating experiments allowed us to follow the crystal to a polymerization of 78%. All evidence tells us that an even slower study would have given us a 100% SCSC polymerization.

Although the polymerization of the terminal aryldiacetylene has taken place in a centrosymmetric crystal, the resulting conjugated polymer is acentric and polar. This might serve as an interesting basis for future applications in nonlinear optics.

Experiments such as these tell us that we have made major progress in our understanding of supramolecular chemistry and crystal design. We can choose a synthetic target and design a synthesis to reach our goal, but along the way there are still plenty of surprises.

**Acknowledgment.** We thank Mr. Andrew Madison for help with some of the model salt preparations. We also thank Prof. Gary P. Halada for the assistance on Raman measurements. We are grateful to the National Science Foundation for support of this research (Grant CHE-0453334).

**Supporting Information Available:** Full experimental details, FTIR and Raman spectra and crystallographic data for each structure discussed in this paper. This material is available free of charge via the Internet at <http://pubs.acs.org>.

JA806663H